Appl. Phys. B 76, 609–612 (2003)
DOI: 10.1007/s00340-003-1147-1

Applied Physics B
Lasers and Optics

S. TZORTZAKIS✉
G. MÉCHAIN
G. PATALANO
M. FRANCO
B. PRADE
A. MYSYROWICZ

Concatenation of plasma filaments created in air by femtosecond infrared laser pulses

Laboratoire d'Optique Appliquée, CNRS UMR 7639, ENSTA – Ecole Polytechnique, Chemin de la Hunière, 91761 Palaiseau Cedex, France

Received: 4 March 2003
Published online: 14 May 2003 •

ABSTRACT We report the first observation of the attachment of two single plasma filaments created collinearly in the atmosphere by IR femtosecond laser pulses. The linked filamentary structure is electrically conductive and emits sub-THz radiation over its entire length. Concatenation is achieved only for a specific time ordering between the two initial laser pulses. The pulse producing the filament closer to the laser source must be retarded with respect to the other pulse. This special time ordering is attributed to the acceleration of light in a self-guided pulse.

PACS 42.25.Bs; 42.65.Jx; 42.65.Re

1 Introduction

Transfer of high laser intensities over long distances through the atmosphere has been a longstanding problem. The initially proposed high-energy nanosecond lasers have shown their limitations very early. The high-density electron plasma produced in air by such pulses prohibits long-range propagation. Typically, disconnected high-density plasma strings are produced by the front of the pulse, which absorb and diffract the rest of the laser beam. In recent years, the propagation of intense ultra-short laser pulses in atmosphere has renewed interest in this problem. For an incident power above a critical value ($P_{cr} \approx 7$ GW for a laser at 800 nm), the femtosecond laser pulse undergoes beam compression along the three dimensions, forming a high-intensity self-guided structure [1–3]. This process is the result of a dynamic balance between two physical mechanisms. The high intensity of the femtosecond pulses leads to self-focusing through the optical Kerr effect. When the on-axis intensity becomes sufficient to ionize the medium, a low-density electron plasma is produced, which reduces the local index of refraction, preventing the collapse of the pulse and restructuring its temporal shape. Filamentation in a restricted sense lasts as long as these two effects compensate.

There are interesting attributes to the self-guided propagation of femtosecond laser pulses. Due to the reduced pulse duration, absorption of laser energy by the plasma it creates is small. This minimizes energy loss via laser–plasma interaction and allows long-range propagation. Furthermore, the highly nonlinear interaction of the pulse with air molecules leads to an important broadening of its power spectrum, giving rise to a continuum emission extending from the UV to the medium infrared. This continuum has been proposed as a source for broadband LIDAR measurements in the atmosphere [4]. Moreover, the weakly ionized air plasma filaments that subside in the trail of the self-guided pulse have been demonstrated to trigger and guide electric discharges, with eventual applications in lightning control [5]. Finally, it has been predicted that such plasma strings should emit intense sub-THz electromagnetic pulses [6]. Very recently, our group has demonstrated experimentally that femtosecond air plasma strings are indeed extended sources of coherent sub-THz radiation [7].

For most applications, including the ones mentioned above, an important aspect concerns the maximum length over which plasma filaments subsist. Self-guided propagation over about 200 m has been clearly demonstrated in horizontal experiments [8]. Vertical propagation experiments in atmosphere suggest the possibility of pulse self-guiding over kilometer distances [4]. In such experiments, the initial laser power greatly exceeds P_{cr}. The laser beam splits into a large number N of randomly distributed filaments, with $N \approx P/P_{cr}$. When the power of individual filaments falls below P_{cr}, they decay by diffraction, restituting most of their energy to a common pool of laser energy, which in turn forms a new multi-filamentary pattern. Successive patterns with a gradually decreasing number of filaments are produced until the reservoir energy is exhausted. The term optical turbulence has been coined to describe this high-power propagation regime [9]. Direct experimental evidence of break-up and fusion of filaments has been reported [10]. However, the question of the maximum length of an individual filament remains unsettled.

In this communication, we report the first experiment showing that it is possible to join two single filaments, effectively increasing their length by more than a factor two. This could provide a route to producing long single filaments using a sequence of shorter ones.

✉ Fax: +33-1/6931-9996, E-mail: stzortz@ensta.fr

2 Experimental

The experiment was performed with a Ti:Sapphire amplified laser system producing 120-fs 800-nm pulses with energies per pulse of up to 30 mJ, operating at 10 Hz. A Michelson-type interferometer divided the initial laser pulse into two secondary pulses with almost equal energies of about 4 mJ. The two pulses were then recombined to a collinear beam, with the possibility of adjusting the time delay between them by using a standard delay line. Two converging lenses, with $f = 3$ m and $f = 4$ m, respectively, were used to introduce different wavefronts to the two pulses. In this way, a collinear sequence of two separated filaments was produced, as schematically depicted in Fig. 1. Filaments had typical diameters of about 100 μm and intensities a few times 10^{13} W/cm^2.

3 Results and discussion

Several different diagnostics were used to follow the filamentation process. Direct evidence of the ionized channel at the trail of a self-guided filament was obtained using the simple electric conduction technique described in [11]. Two electrodes with small holes in their centers were placed in the filaments path. A potential difference of typically 1000 V was applied between the two electrodes separated by 3 cm. In the presence of a conducting channel, the electric circuit was closed. The induced current was monitored across a load resistance of 8.2 kΩ. The ionization curve of each individual filament (A) and (B) was recorded by displacing the circuit along the propagation axis, keeping the inter-electrode distance constant. The corresponding curves are shown in Fig. 2a. Each filament alone left in its trail an ionized channel with nearly homogeneous electron density over its length of about 1 m. The electron density was estimated to be in the range 10^{16}–10^{17} cm^{-3} [11]. The results of Fig. 2a indicate that the two filaments were well separated spatially. The same conductivity measurements could be performed in the presence of both pulses for different initial time delays between them. The results for zero time delay between pulses (A) and (B) are represented by the triangles in Fig. 2b. The two filaments were still essentially disconnected. Similar results were obtained for other time delays except for a specific time ordering. When pulse (A) was retarded by about 100 fs with respect to pulse (B), the two filaments merged into a single one with nearly constant electronic density over a distance ranging from the head of the first filament to the end of the second one, as shown by the squares in Fig. 2b. In the latter case, an enhanced white light continuum was observed visually for the connected filament, as expected from the increased nonlinear interaction length.

Another non-invasive method for measuring the length of a filament is to record the secondary emission from the plasma channel in the sub-THz frequency range. As shown recently [7], femtosecond-laser-produced filaments in air provide extended sources of coherent sub-THz radiation. The sub-THz emission from a plasma string results from the electric dipole moment induced by the radiation pressure force [6]. The dipole moment is oriented along the string axis, leading to radial sub-THz coherent radiation.

A simple heterodyne detection system was used to measure part of the emitted THz radiation. Its spectral detection band could be adjusted to either 94 ± 1 or 118 ± 1 GHz. The detector was placed in a direction perpendicular to the plasma string. Two identical Teflon converging lenses with $f =$ 80 mm were used to image the emission of the plasma string on the detector.

As discussed in more details in [7], the signal obtained by placing the heterodyne detector at different distances along the propagation axis is proportional to the electron density. Thus, recording the THz emission provides a complementary technique for plasma string diagnostics. A comparison between conductivity and THz measurements under similar experimental conditions is shown in Fig. 2a and b, and Fig. 2c and d, respectively. The THz emitting plasma string length was found to be slightly shorter, but the concatenation process was reproduced for the same time delay. Measurements presented here were performed at 94 ± 1 GHz. Comparable signal amplitudes were obtained at 118 ± 1 GHz.

Additional proof of the interconnection of the two filaments can be obtained by studying the beam intensity profile in the intermediate region between the

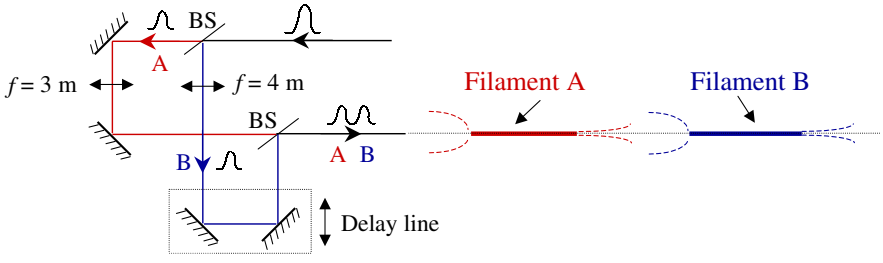

FIGURE 1 Experimental scheme. A Michelson-type interferometer provided a sequence of two collinear pulses. A different curvature was given to each laser beam using two lenses with $f = 3$ and 4 m, leading to the formation of two separated filaments (A and B) in space. An optical delay line controlled the time ordering of the two pulses. BS: Beam Splitter

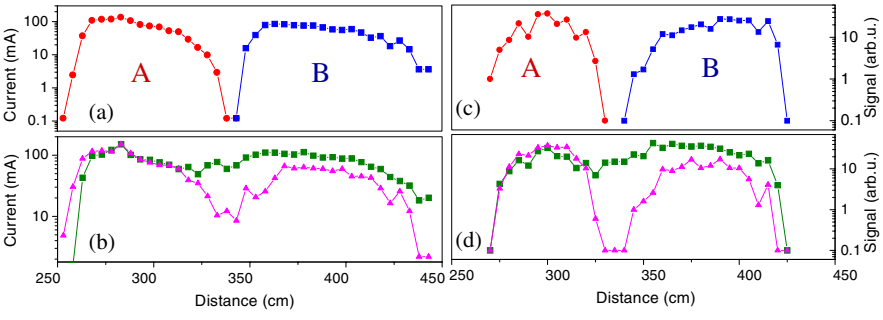

FIGURE 2 Electric conductivity (a), (b) and THz emission at 94 ± 1 GHz (c), (d) measurements along the laser propagation axis. In (a), (c) the *points* were obtained for pulses (A) and (B) launched separately. In (b), (d) the *squares* correspond to $\Delta t = +100$ fs, and the *triangles* to $\Delta t = 0$ fs. A connected filament was observed for $\Delta t = +100$ fs only

two filaments. Due to the high intensities involved, we adopted an indirect experimental technique to visualize the beam intensity profile. A simple glass (BK7) plate oriented perpendicular to the filament axis was introduced in the path at $z = 330$ cm, in the middle of the interconnection region. About 600 shots were accumulated in a run, until an optical damage on the surface of the glass plate was well apparent, which provided information on the beam intensity profile. Measurements were performed for different time orderings between the two initial pulses, using a fresh sample in each run. Subsequent observation of the damage spots shows clear evidence of the interconnection of the two filaments, but again only for $\Delta t = +100$ fs, as shown in Fig. 3b. The filament, due to its high intensity, created a damage track in the bulk (Fig. 3b), while for other delays (Fig. 3a and c) a smaller damage pattern localized on the surface was observed. Notice that surface damage is a highly nonlinear effect and thus only qualitative information is provided by this technique. The damage spot size and shape for the interconnected filament (Fig. 3b) was essentially the same along the entire propagation distance from $z = 250$ to 450 cm.

In order to understand the mechanism linking the two filaments, it is useful to examine the situation at the end of the first filament. For an initial power close to critical, the end of a filament corresponds to a consumption of enough laser energy so that the self-focusing from the optical Kerr effect cannot balance linear and nonlinear diffraction anymore. However, beam divergence is still small, as the power is still near critical. A well-timed second pulse can bring again the total power above P_{cr}. For this energy replenishment to be effective, the timing

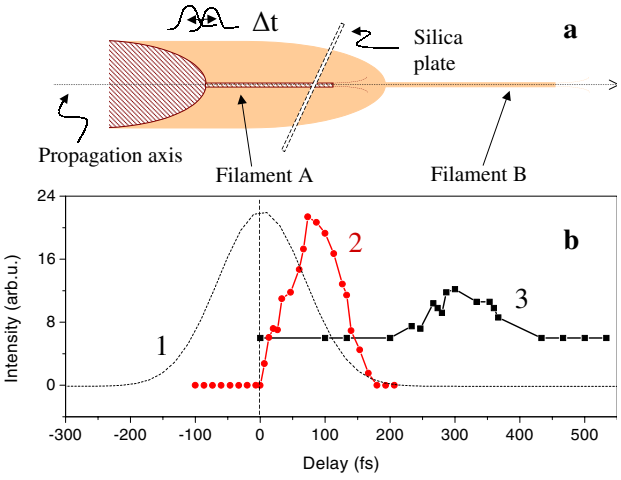

FIGURE 4 **a** A 0.5-mm-thick fused silica plate was placed at $z = 310$ cm at Brewster's angle in the path of filament (A). **b** *Curve 1* represents the second harmonic autocorrelation trace of the initial laser pulses. *Curve 2* corresponds to the THz emission signal measured at $z = 330$ cm as a function of delay between pulses (A) and (B) in the absence of the silica plate. *Curve 3* is the THz signal measured in the presence of the silica plate

of pulse (B) is crucial. In particular, the velocity of the self-guided pulse has to be carefully taken into account.

Numerical simulations give a clue to the origin of the delay. As already mentioned, the filamentation process leads to a considerable reshaping of the pulse profile. From the very early stage of filament formation, highly nonlinear processes such as space–time focusing and ionization conspire to break-up the initial pulse into two sub-pulses with much shorter duration [12–16]. Moreover, our simulations [12] show an acceleration of the dominant leading pulse as it propagates. Typically, for a self-guided propagation in air over 50 cm, the leading pulse is advanced by about 100 fs compared to a normal regime. Similar results have been reported from other groups [13, 16]. It then becomes clear that pulse (A) has to be retarded by about 100 fs for optimal temporal superposition of the two pulses at $z = 320$ cm. Trace 2 in Fig. 4b shows the sub-THz intensity recorded in this intermediate region ($z = 330$ cm) as a function of the delay between pulses (A) and (B). Curve 1 in the same figure corresponds to the second-harmonic autocorrelation trace between the two pulses before propagation. In addition, we note that the retarded trace was narrower. This is consistent with the fact that the signal corresponds to the cross correlation between an initial, undistorted fs pulse and the significantly shorter self-guided pulse.

To confirm our interpretation, we deliberately increased the pulse advance by introducing a thin dielectric plate in the path of the first filament (A). Pulse breaking and acceleration of the leading sub-pulse has also been observed for femtosecond filaments propagating in fused silica [16, 17]. The effect is amplified in a dense medium because of the thousand-fold increase of optical density. For example, a self-guided propagation over 0.5 mm in fused silica is equivalent to 50 cm propagation in air. The experimental scheme is depicted in Fig. 4a. A 0.5-mm thick fused silica plate was placed at Brewster's angle in the propagation path of the two pulses, at $z = 310$ cm. Note that at this position, only pulse (A) propagated in a self-guided mode through the silica plate. The plate was able to withstand the high intensity during a few shots only, after which a rapid deterioration of the filament quality at the plate output was observed. In order to minimize this deleterious effect, the plate was displaced continuously perpendicular to the filament axis. The additional acceleration expected for the self-guided pulse (A) must translate into an increased positive time delay. This was demonstrated by placing the heterodyne detector at $z = 330$ cm and measuring the emitted signal as a function of the time delay

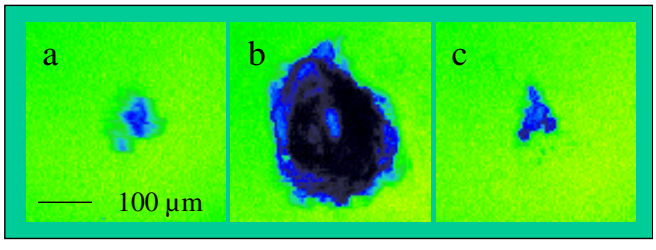

FIGURE 3 Damage impacts of the laser pulses on a glass (BK7) plate, for different time delays, accumulated over 600 shots. The plate was placed at $z = 330$ cm, in the gap between the two filaments. A high intensity filament was obtained only at $\Delta t = +100$ fs, producing bulk damage in the glass (**b**). Limited damage on the surface of the plate was observed at other delays as shown in **a** for $\Delta t = 0$ and in **c** for $\Delta t = -100$ fs

between the two initial pulses. A maximum signal was obtained for a delay of 300 fs, as shown by curve 3 in Fig. 4b. This additional delay is in agreement with theoretical estimates. The discrepancy in the signal amplitude observed between curves 2 and 3 of Fig. 4b is attributed to distortions introduced by the silica plate.

4 Conclusions

In conclusion, we have shown that it is possible to connect femtosecond laser filaments in air. Interconnection of collinear filaments is only possible for a special time ordering of the laser pulses. This effect provides a direct demonstration of the acceleration of light in a self-guided structure. The connected filament leaves a homogenous plasma string in its wake over more than 2 m, and provides an extended one-dimensional source of sub-THz radiation. The principle that has been demonstrated in this communication could find use in applications such as multi-component LIDAR detection or lightning control.

ACKNOWLEDGEMENTS We would like to acknowledge J.-M. Munier, M. Gheudin, G. Beaudin, and P. Encrenaz from the Observatoire de Paris for providing the heterodyne detector, L. Bergé and A. Couairon for fruitful discussions, G. Hamoniaux for his technical assistance, and the CEA/DAM for financial support.

REFERENCES

1 A. Braun, G. Korn, X. Liu, D. Du, J. Squier, G. Mourou: Opt. Lett. **20**, 73 (1995)
2 E.T.J. Nibbering, P.F. Curley, G. Grillon, B. Prade, M. Franco, F. Salin, A. Mysyrowicz: Opt. Lett. **21**, 62 (1996)
3 A. Brodeur, C.Y. Chien, F.A. Ilkov, S.L. Chin, O.G. Kosareva, V.P. Kandidov: Opt. Lett. **22**, 304 (1997)
4 P. Rairoux, H. Schillinger, S. Niedermeier, M. Rodriguez, F. Ronneberger, R. Sauerbrey, B. Stein, D. Waite, C. Wedekind, H. Wille, L. Wöste, C. Ziener: Appl. Phys. B **71**, 573 (2000)
5 M. Rodriguez, R. Sauerbrey, H. Wille, L. Wöste, T. Fujii, Y.-B. André, A. Mysyrowicz, L. Klingbeil, K. Rethmeier, W. Kalkner, J. Kasparian, E. Salmon, J. Yu, J.-P. Wolf: Opt. Lett. **27**, 772 (2002)
6 C.-C. Cheng, E.M. Wright, J.V. Moloney: Phys. Rev. Lett. **87**, 213001 (2001)
7 S. Tzortzakis, G. Méchain, G. Patalano, Y.-B. André, B. Prade, M. Franco, A. Mysyrowicz, J.-M. Munier, M. Gheudin, G. Beaudin, P. Encrenaz: Opt. Lett. **27**, 1944 (2002)
8 B. La Fontaine, F. Vidal, Z. Jiang, C.Y. Chien, D. Comtois, A. Desparois, T.W. Johnston, J.C. Kieffer, H. Pépin, H.P. Mercure: Phys. Plasmas **6**, 1615 (1999)
9 M. Mlejnek, M. Kolesik, J.V. Moloney, E.M. Wright: Phys. Rev. Lett. **83**, 2938 (1999)
10 S. Tzortzakis, L. Bergé, A. Couairon, M. Franco, B. Prade, A. Mysyrowicz: Phys. Rev. Lett. **86**, 5470 (2001)
11 S. Tzortzakis, M. Franco, Y.-B. André, A. Chiron, B. Lamouroux, B. Prade, A. Mysyrowicz: Phys. Rev. E **60**, R3505 (1999)
12 A. Chiron, H.R. Lange, J.-F. Ripoche, B. Lamouroux, M. Franco, B. Prade, A. Mysyrowicz: Eur. Phys. J. D **6**, 383 (1999)
13 O.G. Kosareva, V.P. Kandidov, A. Brodeur, C.Y. Chien, S.L. Chin: Opt. Lett. **22**, 1332 (1997)
14 J.K. Ranka, R.W. Schirmer, A.L. Gaeta: Phys. Rev. Lett. **77**, 3783 (1996)
15 J.K. Ranka, A.L. Gaeta: Opt. Lett. **23**, 534 (1998)
16 A. Zozulya, S.A. Diddams, A.G. Van Engen, T.S. Clement: Phys. Rev. Lett. **82**, 1430 (1999)
17 S. Tzortzakis, L. Sudrie, M. Franco, B. Prade, A. Mysyrowicz, A. Couairon, L. Bergé: Phys. Rev. Lett. **21**, 213902 (2001)